

## Diurnal Variations on a Plasmaspheric Flux Tube: Light Ion Flows and F Region Temperature Enhancements

S. M. Guiter, T. I. Gombosi, and C. E. Rasmussen

Department of Atmospheric, Oceanic and Space Sciences, Space Physics Research Laboratory, University of Michigan

**Abstract.** Diurnal variations on a plasmaspheric flux tube were modelled using a time-dependent, multi-species, one-stream, interhemispheric model for plasmaspheric flows. In the model the coupled time-dependent hydrodynamic equations (continuity, momentum, and energy) of a two ion ( $H^+$  and  $O^+$ ) quasineutral, currentless plasma are solved for a closed geomagnetic field line; no diffusive equilibrium assumptions are made. For this work an  $L = 2$  field line with conjugate points displaced in latitude and longitude was used in order to model the tilt of the geomagnetic field. The simulation was done for June solstice conditions during solar minimum. In general the results reproduce those found by Richards and Torr [1986]. However, a striking new result is the presence of large downward  $H^+$  velocities ( $\sim 2.2$  km/s) at about 320 km altitude in the winter (southern) hemisphere, in early morning when the summer hemisphere is already sunlit but the winter hemisphere is still in darkness. These are accompanied by large  $H^+$  temperature enhancements, reaching 5600 K, at about 280 km altitude. The large velocities are a result of an increase in the  $H^+$  pressure gradient coupled with a decrease in the friction encountered by the  $H^+$  ions. These flows are stopped at lower altitudes where the neutral densities are higher; the bulk kinetic energy is converted to thermal energy, resulting in the temperature enhancements.

## 1. Introduction

Diurnal variations of plasmaspheric flows on field lines whose conjugate points are displaced in latitude and longitude have previously been modelled using codes which make some low speed assumption. For example, Richards and Torr [1986] applied a plasmaspheric flow model, originally developed by Young et al. [1980], for which the inertial terms were neglected, to flows on an  $L = 3$  flux tube in which the winter end was 1.6 hours behind the summer end in local time. They found an upward winter  $H^+$  flux which peaked 1.6 hours in local time before sunrise in the summer hemisphere and several hours before sunrise in the winter hemisphere, due to the strong thermal coupling between conjugate hemispheres which results in heating of  $H^+$  in the winter end. Bailey et al. [1987] used a hydrodynamic model, in which the inertial terms of the momentum equation were neglected, to study the diurnal variation of  $O^+$  fluxes and interhemispheric  $H^+$  fluxes on  $L=1.5$  and  $L=3$  flux tubes for sunspot minimum and medium conditions at June solstice. They found that the conjugate ionospheres were directly coupled for the  $L=1.5$  flux tube but only indirectly coupled on the  $L=3$  flux tube. More recently, Rasmussen et al. [1989] modelled such flows using a three-dimensional, time-dependent hydrodynamic model for which diffusive equilibrium is assumed in the lower ionosphere, but which retains the full continuity and momentum equations above 500 km altitude; however, the lower ionosphere is not self-consistently coupled to the plasmasphere in this model. They found that the tilt of the Earth's magnetic dipole causes annual variations in plasmaspheric density and may explain the annual variations observed by Park et al. [1978].

The purpose of this paper is to report results found modelling flows on a tilted plasmaspheric flux tube using a fully interhemispheric model which does not assume diffusive equilibrium. The model is time-dependent, one-stream and hydrodynamic; it is an adaptation, for closed dipolar field lines, of a polar wind model developed by Gombosi et al. [1985]. This model takes into account the effects of ionization, charge exchange, recombination, collisions, heat conduction, and allows for external heat sources. The model includes heating of electrons due to photoelectrons. The boundaries of the model flux tube are at 200 km altitude. For the study a rotating  $L = 2$  flux tube was used with the northern end at ( $37.7^\circ$  N,  $121.6^\circ$  W) and the southern end at ( $48.9^\circ$  S,  $140.8^\circ$  W). This work was done for June solstice in 1986 (solar minimum), with the result that the southern end was in darkness longer than the northern end. The flux tube was allowed to rotate for several days in order to obtain diurnally reproducible results.

## 2. Model

The model includes the time-dependent coupled continuity, momentum, and energy equations for  $O^+$  and  $H^+$  ions and the energy equation for electrons. As a result of the strong geomagnetic field only motions along magnetic field lines are important; field line curvature effects are neglected. Quasineutrality is assumed and no field-aligned electric currents are allowed. With these constraints one-dimensional forms of the governing equations can be derived; these were presented in an earlier paper [Guiter and Gombosi, 1990].

In this model the collision terms are assumed to have the following form:

$$\frac{\delta M_s}{\delta t} = \sum_t n_s m_s v_{st} (u_t - u_s)$$

$$\frac{\delta E_s}{\delta t} = \sum_t \frac{n_s m_s v_{st}}{m_s + m_t} \left[ 3k (T_t - T_s) + m_t (u_t - u_s)^2 \right]$$

In these equations the summations run over all species;  $v_{st}$  is the momentum transfer collision frequency of species  $s$  with species  $t$ ,  $k$  is Boltzmann's constant,  $n$  is number density,  $m$  is the particle mass,  $T$  is temperature,  $u$  refers to the bulk flow velocity,  $\delta M/\delta t$  is the momentum exchange rate and  $\delta E/\delta t$  is the energy exchange rate. The velocity-dependent correction factors [cf. Tanenbaum, 1967; Burgers, 1969; Schunk, 1977] have been approximated by one. These have been calculated for the cases when there were large downward  $H^+$  velocities; those for collisions with neutral species differ from unity by at most two percent, whereas those for collisions with  $O^+$  ions are less than unity by an amount of 3 to 5 percent.

The neutral atmosphere model used was MSIS-86 [Hedin, 1987]; this includes  $N_2$ ,  $O_2$ ,  $O$ , and  $H$ . For this study the neutral atmosphere was updated every fifteen minutes as the flux tube rotated. As an example, at 300 km altitude in the northern end at 1200 LT (local time at the magnetic equator)  $n(N_2) \sim 6.9 \times 10^7 \text{ cm}^{-3}$ ,  $n(O_2) \sim 2.4 \times 10^6 \text{ cm}^{-3}$ ,  $n(O) \sim 2.5 \times 10^8 \text{ cm}^{-3}$ ,  $n(H) \sim 1.7 \times 10^5 \text{ cm}^{-3}$ , and  $T_n \sim 850\text{K}$ . The  $O^+$  ions are produced by photoionization during the day, whereas the  $H^+$  ions are created by charge transfer only. At night the  $O^+$  photoproduction rate is assumed to be zero; then the only production is due to charge transfer with  $H^+$ .  $O^+$  is removed

Copyright 1991 by the American Geophysical Union.

 Paper number 91GL00139  
 0094-8534/91/91GL-00139\$03.00

by chemical reactions with  $N_2$  and  $O_2$ ;  $H^+$  is removed by charge transfer with  $O$ . The ion-ion, ion-neutral, and ion-electron collision frequencies and the heat conductivities used in this model were taken from Raitt et al. [1975]. The solar zenith angle was found for each cell and for the boundaries and used to calculate the  $O^+$  production rate in each cell; the zenith angles and production rates were updated when the neutral atmosphere was updated. The production rates were calculated using software taken from a conductivity model developed by Rasmussen et al. [1988].

In the model an  $L=2$  flux tube connects two external reservoirs, each at an altitude of 200 km; these reservoirs represent photochemically controlled regions of the ionosphere. The ions in the reservoirs are assumed to be in thermal equilibrium with the neutral atmosphere, while the electron temperature in the reservoirs is assumed to be 1000 K. During the day the ion densities in the reservoirs were determined from photochemical equilibrium; at night the  $O^+$  number density was set at  $1.5 \times 10^3 \text{ cm}^{-3}$ , and the  $H^+$  density determined from the requirement that  $H^+$  be in charge transfer equilibrium with  $O^+$ . The electron volume heat source for altitudes up to 800 km was calculated for various solar zenith angles using the two-stream photoelectron model of Nagy and Banks [1970]; above 800 km this heat source was calculated by assuming that  $\sim 25\%$  of the upward photoelectron energy flux was degraded by interactions with thermal electrons, evenly along the flux tube. For zenith angles greater than  $90^\circ$  the heating rates below 800 km are set to zero but above this altitude a constant heating rate is assumed in order to keep the equatorial temperatures around 3000 K, as observed by Comfort et al. [1985]. In addition a neutral wind profile which is poleward during the day but equatorward at night is assumed; the largest poleward wind was 50 m/s, and the largest equatorward wind was 150 m/s [Crowley et al., 1989]. For this work the model was run assuming solstice conditions during solar minimum (June 21, 1986) and no external ion heating.

The coupled time-dependent partial differential equations are solved using a combined Godunov scheme/Crank-Nicholson method with dimensional splitting.

### 3. Results

Figure 1 shows  $H^+$  particle flux profiles between  $-60$  and  $60$  degrees magnetic latitude for times ranging from 0400 LT to 0530 LT (LT refers to local time at the magnetic equator). Positive latitudes refer to the northern hemisphere. It should be noted that positive flows are upward in the northern hemisphere but downward in the southern hemisphere. At 0400 LT the  $H^+$  flows down in both hemispheres. At 0430 LT the sun has risen in the northern hemisphere; at this time there are upward  $H^+$  fluxes in the northern hemisphere, and in the southern hemisphere above 2000 km altitude. There are upward fluxes in both hemispheres because both are heated,

by photoelectrons and by heat conduction from the plasmasphere which is heated by escaping photoelectrons; this increases the scale heights in the ionospheres which means that the ionospheres are expanding. The upward flux in the northern hemisphere is a perturbation which moves toward the southern ionosphere, reaching it at about 0450 LT. This perturbation propagates at  $\sim 8.3 \text{ km/s}$ , which is roughly the ion-acoustic speed. After this time flux waves propagate between the ends, as can be seen from 0500 LT to 0520 LT. By 0530 LT the waves have decayed and the flux profile is very similar to that seen at 0600 LT.

Figure 2 shows flux and temperature profiles for  $H^+$  and  $O^+$  ions at 0600 LT, 1200 LT, 1800 LT, and 2400 LT. At 0600 LT the northern end is sunlit but the southern end is still in darkness. From the  $H^+$  flux profile it can be seen that  $H^+$  is flowing from the northern to southern hemispheres. In addition, the  $H^+$  flux in the southern hemisphere is about twice that in the northern hemisphere, as the  $H^+$  ions are accelerated downward. The velocity profile shows that there is a large downward  $H^+$  velocity in the southern hemisphere at about 320 km altitude with a maximum speed of about 2.2 km/s (see Figure 3). This feature is accompanied by a large enhancement in the  $H^+$  temperature (to about 5600 K) in the southern hemisphere at about 280 km altitude.

The strong downward  $H^+$  velocity is the result of an increase of the pressure gradient coupled with a large decrease in the friction encountered by the  $H^+$  ions. During the day the  $H^+$  pressure gradient force, which is downward, is balanced by the polarization electric field which is upward and friction due to Coulomb collisions with  $O^+$  ions, resulting in low velocities. At night the  $H^+$  pressure gradient increases by a factor of two due to a reduction in the equilibrium  $H^+$  density at lower altitudes, brought about by a decrease in the  $O^+$  density at those altitudes. In addition, the electric field term in the momentum equation is an order of magnitude smaller than the pressure gradient term. However, the momentum transfer collision frequency of  $H^+$  ions with  $O^+$  ions [ $\nu(H^+, O^+)$ ] does not decrease significantly, because of the lower  $H^+$  temperatures at those altitudes and the maintenance of the  $O^+$  densities by the equatorward neutral winds. This results in only moderate downward  $H^+$  velocities at both ends.

This changes significantly at 0430 LT when the sun rises in the northern hemisphere. At this time  $T(H^+)$  in the southern ionosphere rises due to heating by photoelectrons from the northern hemisphere and heat conduction from the plasmasphere which is also heated by photoelectrons. This significantly decreases  $\nu(H^+, O^+)$  which leads to a rise in the downward  $H^+$  velocity. Then because of the conversion of kinetic energy to thermal energy at lower altitudes the  $H^+$  temperature increases, which results in a further decrease of  $\nu(H^+, O^+)$ . This results in a further increase of the downward  $H^+$  velocity, setting up a positive feedback effect. This can be seen in Figure 3, which shows altitude profiles of the  $H^+$  velocity and temperature and of  $\nu(H^+, O^+)$  in the southern hemisphere from 0300 LT to 0600 LT at half-hour intervals.

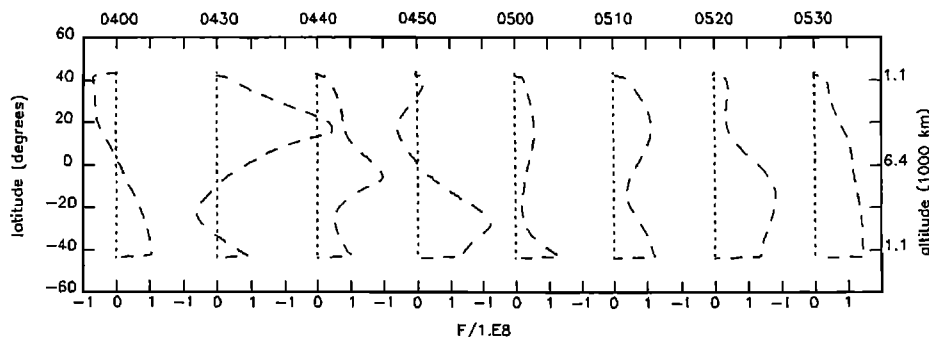


Fig. 1:  $H^+$  flux profiles between  $-60$  and  $60$  degrees magnetic latitude for 0400 LT to 0530 LT (local time at the magnetic equator).

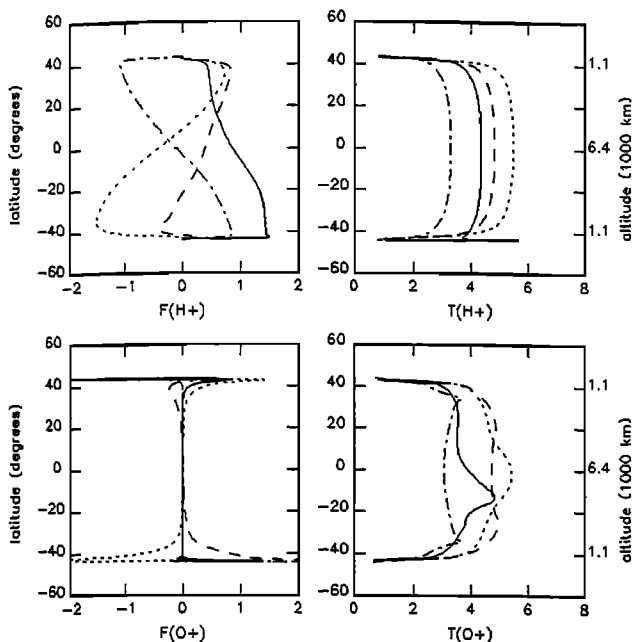


Fig. 2: Particle flux (normalized to a reference altitude of 1000 km) and temperature profiles for H<sup>+</sup> and O<sup>+</sup> ions between -60 and +60 degrees magnetic latitude. Solid lines refer to profiles at 0600 LT, dotted lines correspond to those at 1200 LT, dashed lines refer to those at 1800 LT, and dot-dashed lines refer to those at 2400 LT.

Note that  $v(H^+,O^+)$  decreases with time whereas the velocity and temperature increase with time.

By 0600 LT  $v(H^+,O^+)$  has decreased enough so that the H<sup>+</sup> ions can only be stopped by collisions with neutral species (although this does not mean that Coulomb collisions are unimportant), which stops the positive feedback effect. Since the momentum transfer collision frequency of the H<sup>+</sup> ions with the neutral species is an order of magnitude smaller than that with the O<sup>+</sup> ions during the day, the H<sup>+</sup> ions experience very little friction. The increased pressure gradient is not balanced by the electric field and can only be balanced by the friction terms if there are large downward velocities. At lower altitudes the neutral densities are large enough so that there is enough friction to stop the flow. The bulk kinetic energy is then converted to thermal energy, resulting in the large H<sup>+</sup> temperature enhancement.

At 1200 LT the entire flux tube is sunlit. There are upward flows of H<sup>+</sup> ions in both ionospheres, as shown in the H<sup>+</sup> flux profile; there is also a flow out of the southern (winter) hemisphere into the northern (summer) hemisphere. In addition, there is a dip in the H<sup>+</sup> density at about 1000 km

altitude in the southern hemisphere (density profile not shown), caused by the strong outflow of H<sup>+</sup> from this region.

At 1800 LT the northern end is still sunlit but the southern end is going into darkness. Again there are upward flows of H<sup>+</sup> ions in both ionospheres, but now there is a net flow out of the northern ionosphere into the southern hemisphere. Also, from the temperature profiles it can be seen that the equatorial temperatures have decreased relative to those at 1200 LT.

At 2400 LT the entire flux tube is in darkness. The flux profiles show that there is a downward H<sup>+</sup> flux in each hemisphere. There are also small downward H<sup>+</sup> velocities in both hemispheres, at about 410 km altitude in the northern end and at about 425 km altitude in the southern end (velocity profiles not shown).

#### 4. Summary

As a summary of our results, Figure 4 shows the upward H<sup>+</sup> flux profiles in the northern and southern hemispheres at 3000 km altitude as a function of the local time in each hemisphere. It should be noted that the local time in the northern hemisphere is ~ 22 minutes later than the local time at the magnetic equator, while the local time in the southern hemisphere is ~ 25 minutes before. The key points are as follows. From midnight to 0400 there are downflows in both hemispheres due to the emptying of the plasmaspheric reservoir. When the sun rises in the northern end there are upflows in both hemispheres (points A and A'). The upflow in the southern hemisphere precedes (in local time) that in the northern because the southern end is earlier in local time (but at the same universal time). After the northern sunrise the upward flux perturbation travels from the northern to southern hemispheres; this can be seen in the transients following the upflows. At about 0800 the sun rises in the southern hemisphere, leading to an upflow in the southern hemisphere (point B). Following this there are transients due to flux waves propagating between the ends; these are especially prominent in the northern hemisphere. During the day there are upward fluxes in both hemispheres; the flux in the southern hemisphere is larger than that in the northern because of the larger H<sup>+</sup> pressure in the southern reservoir. At approximately 1630 the sun sets in the southern hemisphere, leading to downflows in both hemispheres (points C and C'). The downflow in the southern hemisphere is due to the dropoff in the photoelectron heating below 800 km altitude, leading to lower ionospheric pressures. The initial downflow is part of a flux wave which travels between the hemispheres, leading to the quick return to upward flux following the downflow. At about 1930 the sun sets in the northern hemisphere, leading to strong downflows in both hemispheres (points D and D'). The initial downflow is a perturbation which travels toward the southern hemisphere, leading to the quick return to smaller fluxes and the transients which follow.

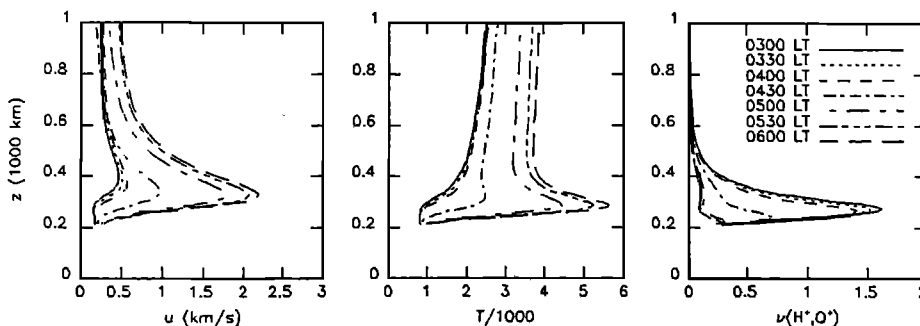


Fig. 3: Altitude profiles of H<sup>+</sup> velocity and temperature and of  $v(H^+,O^+)$  in the southern hemisphere from 0300 LT to 0600 LT at half-hour intervals.

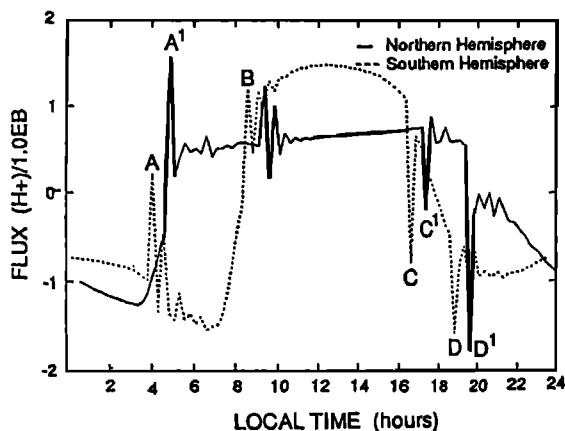


Fig. 4: Upward  $H^+$  flux profile at 3000 km altitude in the northern and southern hemispheres as a function of the local time in each hemisphere.

The most striking result occurs at 0600 LT when the southern end is in darkness. At such times large downward  $H^+$  velocities ( $\sim 2.2$  km/s) are seen at about 320 km altitude accompanied by a large  $H^+$  temperature increase (reaching 5600 K) around 280 km altitude. In addition, an upward  $H^+$  flux is seen in the southern hemisphere at altitudes above 2000 km when the sun rises in the northern end; however, this is much more transient than that obtained by Richards and Torr [1986], due to the flux perturbation which travels from the northern to southern hemispheres. In general, the diurnal variation of the upward  $H^+$  flux at 3000 km altitude resembles that of Richards and Torr [1986]; important differences include the transients following sunrise and sunset, the strong downflows at local and conjugate sunset, and the downflows in the northern hemisphere during the night. In addition, the diurnal variation of the  $O^+$  flux at 1000 km altitude roughly agrees with that of Bailey et al. [1987] for solar minimum at  $L = 1.5$ ; at 500 km there is resemblance only in the evening. Our interhemispheric  $H^+$  flux changes sign, whereas that of Bailey et al. [1987] is always from north to south.

The photoelectron heating rates used in the model were calculated under the assumption that the downward photoelectron flux at 800 km altitude is roughly 70% of the upward photoelectron flux at that altitude. While this is appropriate during the day it is probably not at sunrise, which means that the photoelectron heating profiles could be too high then. However, the plasmaspheric heating would still increase at sunrise and so the positive feedback effect leading to the large  $H^+$  velocities could still occur.

**Acknowledgements.** This work was supported by NSF grant ATM-8908183 and NASA grant NAGW-2162. One of us (SMG) was supported by NASA Marshall Space Flight Center through the graduate student training grant NGT-50368. Acknowledgement is also made to the National Center for Atmospheric Research, sponsored by the National Science Foundation, for the computing time used in this research.

## References

- Bailey, G. J., P. A. Simmons, and R. J. Moffet, Topside and interhemispheric ion flows in the mid-latitude plasmasphere, *J. Atmo. Terr. Phys.*, 49, 503, 1987.
- Burgers, J. M., *Flow Equations for Composite Gases*, Academic, New York, 1969.
- Comfort, R. H., J. H. Waite, Jr., and C. R. Chappell, Thermal ion temperatures from the retarding ion mass spectrometer on DE 1, *J. Geophys. Res.*, 90, 3473, 1985.
- Crowley, G., B. A. Emery, R. G. Roble, H. C. Carlson, Jr., J. E. Salah, V. B. Wickwar, K. L. Miller, W. L. Oliver, R. G. Burnside, and F. A. Marcos, Thermospheric dynamics during September 18-19, 1984, 2, Validation of the NCAR thermospheric general circulation model, *J. Geophys. Res.*, 94, 16,945, 1989.
- Gombosi, T. I., T. E. Cravens, and A. F. Nagy, A time-dependent theoretical model of the polar wind: Preliminary results, *Geophys. Res. Lett.*, 12, 167, 1985.
- Gutter, S. M., and T. I. Gombosi, The role of high speed plasma flows in plasmaspheric refilling, *J. Geophys. Res.*, 95, 10,427, 1990.
- Hedin, A. E., MSIS-86 thermospheric model, *J. Geophys. Res.*, 92, 4649, 1987.
- Nagy, A. F., and P. M. Banks, Photoelectron fluxes in the ionosphere, *J. Geophys. Res.*, 75, 6260, 1970.
- Park, C. G., D. L. Carpenter, and D. B. Wiggin, Electron density in the plasmasphere: Whistler data on solar cycle, annual, and diurnal variations, *J. Geophys. Res.*, 83, 3137, 1978.
- Raitt, W. J., R. W. Schunk, and P. M. Banks, A comparison of the temperature and density structure in the high and low speed thermal proton flows, *Planet. Space Sci.*, 23, 1103, 1975.
- Rasmussen, C. E., R. W. Schunk, and V. B. Wickwar, A photochemical equilibrium model for ionospheric conductivity, *J. Geophys. Res.*, 93, 9831, 1988.
- Rasmussen, C. E., J. J. Sojka, and R. W. Schunk, Modeling of annual variations in plasmaspheric density, AGU Fall Meeting, San Francisco, CA; *EOS Trans.*, AGU, 70, 1247, 1989.
- Richards, P. G., and D. G. Torr, Thermal coupling of conjugate ionospheres and the tilt of the Earth's magnetic field, *J. Geophys. Res.*, 91, 9017, 1986.
- Schunk, R. W., Mathematical structure of transport equations for multispecies flows, *Rev. Geophys. Space Phys.*, 15, 429, 1977.
- Tanenbaum, B. S., *Plasma Physics*, McGraw-Hill, New York, 1967.
- Young, E. R., D. G. Torr, P. Richards, and A. F. Nagy, A computer simulation of the midlatitude plasmasphere and ionosphere, *Planet. Space Sci.*, 28, 881, 1980.

S.M. Gutter, T.I. Gombosi, and C.E. Rasmussen, Department of Atmospheric, Oceanic and Space Sciences, Space Physics Research Laboratory, 2455 Hayward, Ann Arbor, Michigan 48109-2143.

(Received November 12, 1990;  
accepted January 10, 1991)